

# Design of a new expendable profiler, XMS (Expendable Multiple Sensor)

Hiroki Hei \*, Hiroki Yasuma \*\*, Kazuyoshi Maekawa\*\*,  
Yasuzumi Fujimori\*\*, and Nobuo Kimura\*\*

\* Graduate School of Fisheries Sciences, Hokkaido University, Japan

\*\* Faculty of Fisheries Sciences, Hokkaido University, Japan

## Abstract

The authors designed the body shape of XMS (Expendable Multiple Sensor) for oceanographic research. XMS was required to achieve the same performance as XBT (Expendable Bathy Thermograph) and fall without rotation. CFD analysis was conducted to obtain the optimal design in considering minimizing drag without body rotation in the water. Additionally, the falling test on the sea was conducted to confirm the performance of XMS body by the mock-up model based on the CFD result. In the experiment, the mock-up model fell stably without rotation. Moreover, the falling velocity was over that of XBT. From these results, it is concluded that the optimal shape of XMS was designed.

Keywords: CFD, XBT, hydrodynamics

## 1 Introduction

The XBT (Expendable Bathy Thermograph) make it possible to obtain the profiler of the water temperature over a wide range in a short time, and it is used widely in oceanographic studies. However, some environmental concerns have been pointed out on the existent XBT. For example, the lead sinker and the plastic body would cause water pollution. Technical improvements are also required to the multiple measurements, because the existent XBT can install only one (temperature) or two (temperature and salinity) sensors due to its size limitation.

Therefore, we have been developing a new expendable instrument for the multiple measurements, named XMS (Expendable Multiple Sensor). The XMS will consist of biodegradable plastic body and steel sinker, and the XMS needs to be relatively large

size that it can install various sensors such as the depth, salinity, and image data. These characteristics of the size and the materials in the XMS can be major effects on the condition of falling into the sea. The biodegradability materials planned to use in this study has lower density than the plastic used in the existent XBT, and the steel sinker is lighter than the lead sinker. The large body size would cause the larger drag effect. These factors should be considered to design the shape of the XMS to achieve the same performance as the XBT. Additionally, the XMS must fall without rotation unlike XBT to obtain the image data, and prevent twisting of the signal line which is thicker than that of XBT.

In this study, we designed the shape of XMS using CFD (Computational Fluid Dynamics) analysis so as to minimize the drag and prevent the rotation. Moreover, the falling test on the sea was conducted to confirm the performance of the XMS designed using the mock-up model based on the CFD result.

## 2 METHOD

### 2.1 CFD analysis

#### 2.1.1 Base Model

Model shape of the XMS was determined as below, based on Tetsumura et al.<sup>[1]</sup>

- 1) The total length of the profiler is 25.0 cm, the maximum radius is 3.3 cm, and the radius of the rear end is more than 1.1 cm. These values are determined to have enough volume to install multiple sensors.
- 2) Providing two ditches to expose sensors outside, so as not to interrupt the flow of water.
- 3) The profiler has spheroidal head to reduce drag.
- 4) Attaching four fins to prevent the rotation of the body and the signal line.
- 5) The falling velocity must be over 6.0 m/s to achieve the same performance of XBT.

An overview of the Base Model and the coordinate system in this study are shown in Fig. 1. Ditches placed in the model are shown in Fig. 2.

The shape of the Base Model (without fins) was changed to reduce the drag and fall stably by changing geometry parameters shown in Fig. 3. Parameter  $a$  was the length of the long axis of the spheroidal head. Parameter  $b$  was region of the spheroidal, in which  $b$  was longer than  $a$ . The  $d$  and  $r$  (the radius of a quarter circle) represented the size of the rear end. The parameters of Base Model are shown in Table 1. After the analysis, the fins were attached to the optimal model to prevent its rotation as shown in Fig. 4. Then, XMS is required to fall as fast as XBT, a general expendable sensor. The usual falling velocity of XBT is about 6.0 m/s<sup>[2]</sup>, however, we must take into account the drag of the signal lines. Therefore, in order to achieve the falling velocity more than 6.0 m/s, the

inflow velocity set as 7.5 m/s in CFD analysis.

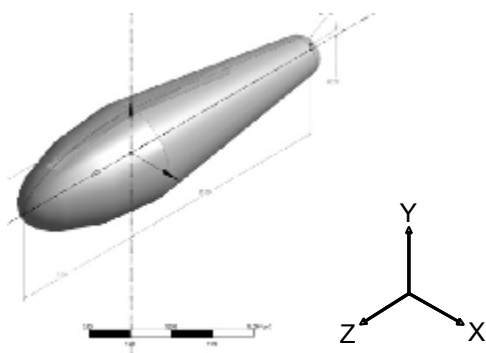


Fig. 1 Overview of the Base Model and the coordinate system

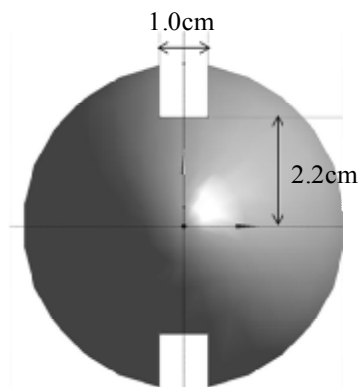


Fig. 2 Ditches in the model

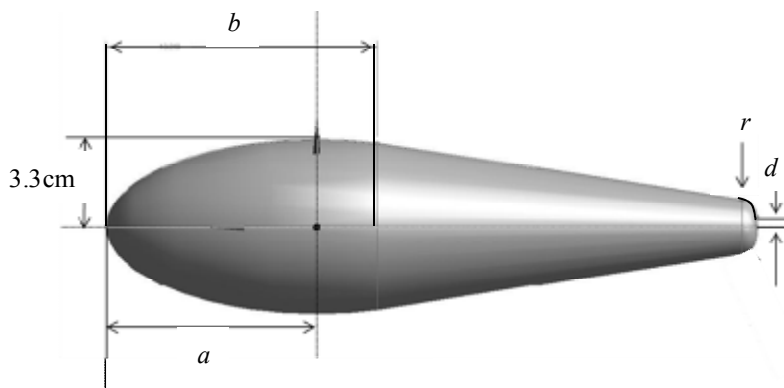


Fig. 3 Definition of the body parameter

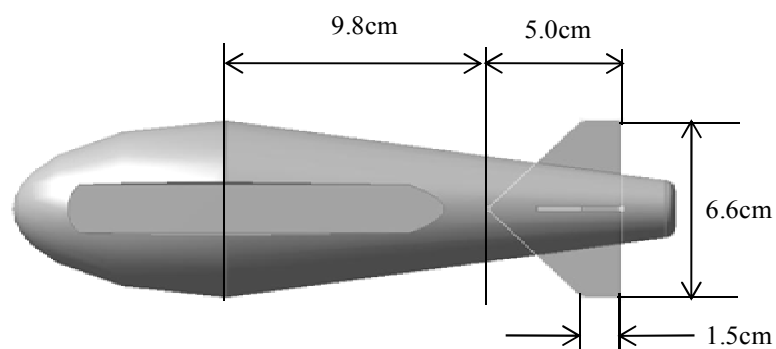


Fig. 4 Design of the fins for preventing rotation of the body

Table 1 The value of parameters on the Base Model

Model	$a$ [cm]	$b$ [cm]	$d$ [cm]	$r$ [cm]
Base	9.0	9.0	0.4	1.0

### 2.1.2 Method of analysis

The fluid analysis software ANSYS (CYBERNET Inc.) was used to estimate the drag of the XMS and the distribution of the flow around it. The calculation was conducted to

solve the Navier-Stokes equations and the continuity equation that were basic equations of the flow by the finite volume method <sup>[3]</sup>, under the turbulence model called SST (Shear Stress Transport) model. The tetrahedron mesh was used and number of the element was about 500 thousand. Domain of calculation was a cube 2.0 m on a side. And the model was located in the center. In the boundary condition shown in Fig. 5, there was no slip on the model surface and the inflow velocity of the fluid was set at 7.5 m/s, relative pressure was 0 Pa in the out and opening flow. In the computational condition, the kind of the fluid was set as water, the water density was 997 kg/m<sup>3</sup>, the water temperature was 25.0 degree Celsius, viscosity was 8.899×10<sup>-4</sup> kg/ms, and kinematic viscosity was 0.893×10<sup>-6</sup>m<sup>2</sup>/s.

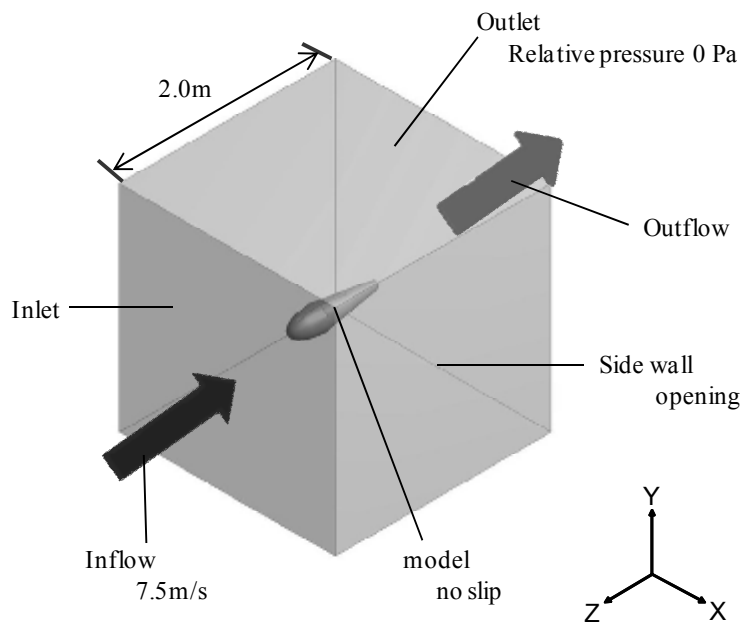


Fig. 5 Computational domain of the fluid analysis

## 2.2 Falling test

A mock-up model based on the optimal model obtained by CFD analysis was made to falling test in the sea. Figure 6 shows the overview of the mock-up model. The weight was 1.28 kgf, and the volume was 424.51 cm<sup>3</sup>. The head of the model was made from steel, and the body was plastic. The weight of the model was calculated so that falling velocity was kept to be 6.0 m/s or more, using a motion equation and terminal velocity of the model.

$$W \frac{dU}{dt} = (W - \rho V)g - \frac{1}{2} C_D A \rho U^2 \quad (1)$$

$$U_{\infty} = \sqrt{\frac{2(W - \rho V)g}{C_D A \rho}} \quad (2)$$

Equation (1) is the motion equation of the mock-up model and  $U_{\infty}$  in equation (2) is the terminal velocity of the model. Here,  $W$  is mass of the mock-up model,  $\rho$  is density of fluid,  $V$  is volume,  $g$  is acceleration of gravity,  $C_D$  is drag coefficient,  $A$  is projected area, and  $U$  is falling velocity.

The model was filled with oil clay to become the weight calculated from the equations. Then, a data logger (DST Pitch and Roll /star oddi Inc.) was set in the model to measure the water depth, pitch angle, and roll angle while falling. The pitch angle was defined as rotation around  $x$ -axis, and the roll angle as rotation around  $z$ -axis. The pitch angle was regarded  $z$ -axis direction as  $90.0^{\circ}$ . The coordinate system was shown in Fig. 1 and Fig. 5.

The falling test was conducted using a research vessel “Ushiomaru (179GT)” at the depth about 60m, off the coast of Matsumae, Hokkaido in December 22, 2010. The mock-up model was suspended by hanging line (0.403mm in diameter) and electric reel on a fishing rod. The hanging line corresponded to the signal line in actual XMS. The model was set at the sea surface, and keeping motionless for a moment, and then dropped to 40-50m with free tension. The water depth, pitch angle, and roll angle of the model through the falling were measured every second by the logger inside the model. This process was repeated four times, and the logger was ejected from the model to retrieve the recorded data.



Fig. 6 Overview of the mock-up model

## 3 Result

### 3.1 CFD analysis

The estimated drag effect of the Base Model was 7.2N, and the lowest drag effect

(6.8N) was gotten when the parameters  $a = 8.0$ ,  $b = 8.0$ ,  $d = 0.4$ , and  $r = 0.7$  (defined as the Model A later). Pressure distribution of Model A is shown in Fig. 7. The effect of validation in  $a$  on decreasing of the drag was 0.1N at maximum, and validation in  $b$  was thought to be negligible. On the other hand, increasing in  $d$  and  $r$  led to large change of drag value (0.3N at maximum), implying that slim end (as Model A) was effective for decreasing of the drag.

In Fig. 7, the pressure on the whole body was small except for the front of the body, and the rear end was not so high. Moreover, there were no difference of pressure between near the ditch and the other body surface. Also the pressure inside the ditches was almost the same with the pressure on the body. Thus, it seems that the sensors exposed in ditches can exactly measure hydraulic pressure and so on in actual measurement. Therefore, the fins were attached to Model A as the optimal model in the analysis. Moreover, the shape of the ditches was changed to meet the request of the production. This model was called Model B. The front view of the Model B is shown in Fig. 8. The analysis of Model B was conducted to estimate the effect of attaching fins and changing of ditches.

The drag and details of Model B are shown in Table 2 and a pressure distribution of Model B is shown in Fig. 9, and a streamline of Model B is shown in Fig. 10. The decrease of the drag by changing the ditches from Model A (without the fins) was 0.3N. The increase of the drag by attaching the fins was 3.9N, and so the fins accounted for 40 percent of the total drag. As shown in Fig. 9, there was almost no difference between Model A and B in the pressure distribution. This is also the same on inside of ditches. On the fins, there was the same pressure of the body, and so it seems to prevent the rotation of the profiler. As shown in Fig.10, the flow on the Model B was thought to be smooth and stable since there was no separation of the flow on the surface. Therefore, Model B was regarded as the optimal model, and the falling test was conducted in this model.



Fig. 7 Pressure distribution of the Model A

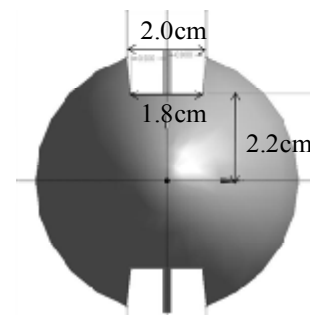


Fig. 8 Front view of the model after change

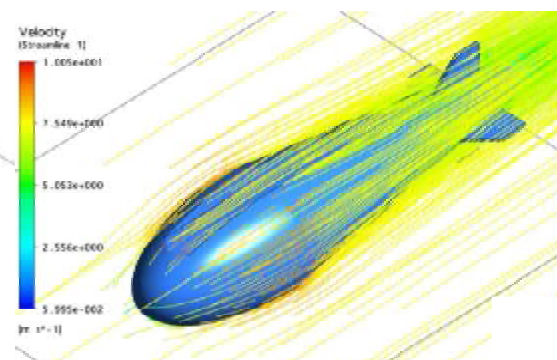
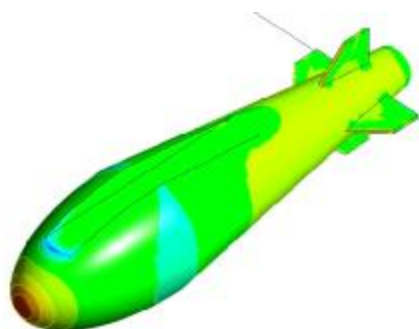
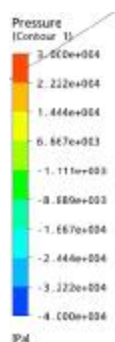


Fig. 9 Pressure distribution of the Model B

Fig. 10 Streamline of the Model B

Table 2 The drag and details of the Model B

Model	Drag [N]	Projected area [cm <sup>2</sup> ]	Volume [cm <sup>3</sup> ]
B	10.4	30.0	424.5

### 3.2 Experiment

The weight calculated by equation (1) and (2) was 1.5 kgf. The validation of falling velocity, the roll angle, and the pitch angle with time are shown in Fig. 11, Fig. 12 and Fig. 13, respectively. The falling velocity was calculated from the validation of the water depth of the mock-up model. Therefore, it is considered that the falling velocity was decreased by the motion of the research vessel and the wave force, the maximum value of the falling velocity was treated as the terminal velocity and it is shown in Table 3.

As shown in Fig. 11, the falling velocity of the mock-up model became stably within about 1.0-2.0 s, and it was kept at 5.0-6.0 m/s after 3 s. The terminal velocity reached to 6.4 m/s on average, thus the mock-up model achieved the required velocity of falling. In Fig. 12, the roll angle became 15.0° in the 1st measurement. The roll angle became about 20.0° after the start of falling, and finally it became nearly 0.0° in the 2nd-4th measurement. Therefore, the model fell without rotation. In Fig. 13, the pitch angle indicated 30.0° and became 90.0° gradually. The large variation was observed until 1.0-3.0 s, after that the model was attained stable.

Table 3 The terminal velocity of the mock-up model

Measurements	1st	2nd	3rd	4th	Average
U <sub>max</sub> (m/s)	6.9	6.4	6.4	6.0	6.4

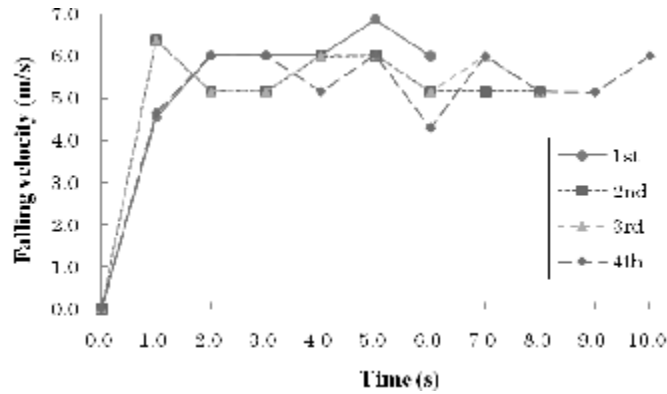


Fig. 11 The falling velocity of the mock-up model and time

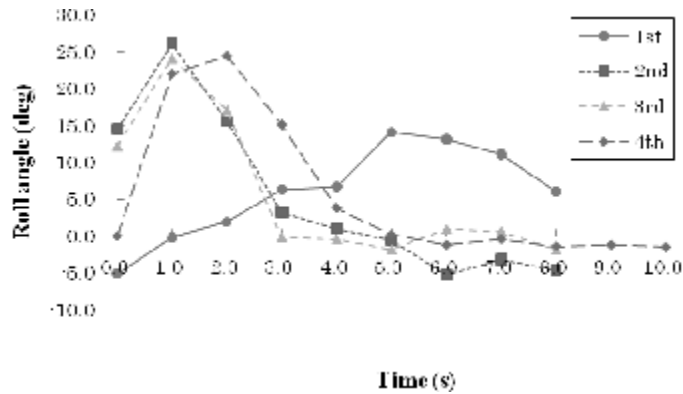


Fig. 12 Relationship between roll angle of the mock-up model and time

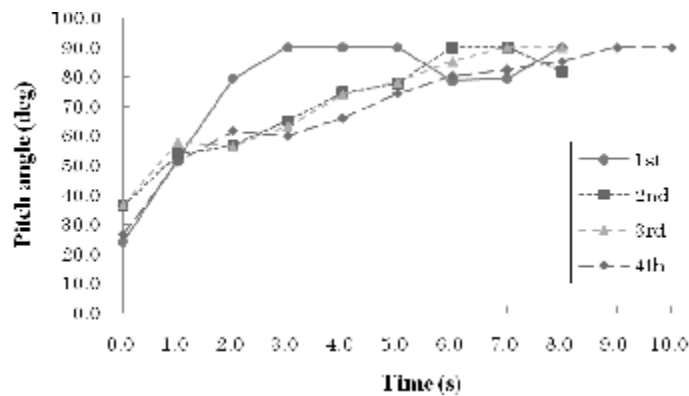


Fig. 13 Relationship between pitch angle of the mock-up model and time

## 4 Conclusion

The little difference of the drag was observed with changing parameter  $a$  and  $b$ . It was considered that the drag depended on the projected area. Since there was no relation between projected area and the parameters  $a$ ,  $b$ , the validation of the drag was little. The decrease of the drag was shown when the shape of the rear end represented by



parameter  $d$  and  $r$  became slender. Hence, it seems that the flow becomes smooth around thinner shape of rear end. The pressure distribution around Model A was stable even with the ditches, and that of Model A and B became the same. Moreover, the smooth flow was observed inside the ditches (in which sensors will be set) of Model B, which allows proper measurements at the depth. The fins seemed to prevent the rotation, however, the drag was very large. The fins cannot be thinner than this, since the biodegradability material is frail. If the falling velocity is required to become faster than the mock-up model, it is the tasks for the future.

In the falling experiment, the falling velocity of the mock-up model (6.4 m/s) was lower than estimated value of CFD analysis (7.5 m/s). Though the cause of this difference is unclear, hanging line and/or the gap at the junction between the head and body would have a certain effect on the drag. However, sufficient falling velocity (same as the XBT) could be obtained in the XMS developed in present study. The rotation and instability of pitch angle were observed in 1.0-3.0 s, however, they were not observed after 3.0 s. It is considered that they were caused by the wave of surface layer. Therefore, the model fell smoothly without rotation, since the roll and pitch angle became optimal in time. From these results, it is concluded that the shape has low drag and falls smoothly without rotation. Therefore, we designed the optimal shape of XMS by CFD analysis and falling test in this study.

## References

- [1] Kotaro TETSUMURA et al.: Design of a New Type of XBT Profiler by the CAE Technique, Mathematical and Physical Fisheries Science vol.7, 43-51, 2009.
- [2] Takahiro MIURA: Depth error in time-depth equations of the T-5 XBT probes, Technical reports of Japan Marine Science and Technology Center, Vol. 49, 73-80, 2004.
- [3] Kazue Onishi: Flow analysis by computer, Asakura Syoten, 1988.
- [4] Akira Goto et al.: Hydrodynamic design system for pumps based on 3-D CAD, CFD, and inverse design method, Journal of Fluid Engineering, vol. 124, 329-335, 2002.

Received  
Accepted

## Academic backgrounds:

### **Hiroki Hei**

04/2007 – 03/2011 Faculty of Fisheries Hokkaido University, Japan  
04/2011 – Master's course of Graduate School of Fisheries  
Hokkaido University, Japan

### **Hiroki Yasuma**

04/2004 – 03/2010 Postdoctoral Fellow, Field Science Center for the  
Northern Biosphere, Hokkaido University, Hokkaido,  
Japan  
04/2010 – 03/2011 Researchers, Fisheries Technology Department, Kyoto  
Prefectural Agriculture, Forestry and Fisheries  
Technology Center, Kyoto, Japan  
04/2011 – Associate Professor, Hokkaido University, Japan

Research field: Fishery acoustics, Mesopelagic community

### **Kazuyoshi Maekawa**

04/1993 – Assistant Professor, Hokkaido University .Japan

Research field: Dynamics and control of fishing vessel, Hydrodynamics

### **Yasuzumi Fujimori**

04/1994 – 03/2005 Assistant Professor, Hokkaido University, Japan  
04/2005 – 04/2010 Associate Professor, Hokkaido University, Japan  
05/2010 – Professor, Hokkaido University, Japan

Research field: Fishery process and the selectivity of fishing  
implements

### **Nobuo Kimura**

04/1986 – 03/1991 Assistant Professor, Hokkaido University, Japan  
04/1991 – 03/2005 Associate Professor, Hokkaido University, Japan  
04/2005 – Professor, Hokkaido University, Japan

Research field: Seakeeping quality of fishing vessel, Fishing  
Engineering, Fluid dynamics